

# Collective Cell Movement in Primary Melanoma Explants: Plasticity of Cell-Cell Interaction, $\beta$ 1-Integrin Function, and Migration Strategies<sup>1,2</sup>

Yael Hegerfeldt, Miriam Tusch, Eva-B. Bröcker, and Peter Friedl<sup>3</sup>

Department of Dermatology, University of Würzburg, 97080 Würzburg, Germany

## ABSTRACT

Collective cell movement represents an efficient dissemination strategy in neoplastic epithelial and mesenchymal cancer. In primary melanoma explants cultured in three-dimensional collagen lattices, invasive migration of multicellular clusters was dependent on the function of  $\beta$ 1-integrins, as shown by preferential  $\beta$ 1-integrin expression and clustering in a subset of promigratory cells at the leading edge (“guiding cells”) and the abrogation of multicellular migration by adhesion-perturbing anti- $\beta$ 1-integrin antibody. Interference with  $\beta$ 1-integrin function induced complex changes in cluster polarity and cohesion, including development of two or several opposing leading edges, cluster disruption, and the detachment of individual cells followed by  $\beta$ 1-integrin-independent “amoeboid” crawling and dissemination. The conversion from  $\beta$ 1-integrin-dependent collective movement to  $\beta$ 1-integrin-independent single-cell motility suggests efficient cellular and molecular plasticity in tumor cell migration strategies.

## INTRODUCTION

Tumor cell invasion into interstitial tissue is a complex process that includes the migration of individual cells as well as multicellular, collective cell movement (1, 2). Collective cell movement, *i.e.*, the migration of cell sheets, aggregates, or clusters, is relatively common in higher eukaryotes, as described previously for two-dimensional sheets of keratinocytes (3), fish melanocytes (4), and adenocarcinoma cells (5); the *in vivo* movement of cell groups in embryological development (6–8); and the migration of cell clusters from tumor explants cultured in three-dimensional collagen lattices (9).

To understand the development of different migration programs in tumor cell invasion and motility, it is important to dissect cellular and molecular similarities and differences among individual and collective cell movements (10, 11). Both migration strategies are dependent on front-rear asymmetry driven by a dynamic leading edge and coordinated detachment of the trailing edge (1, 9). In two- and three-dimensional models for individual tumor cell migration, anterior force generation is provided by adhesion receptors of the integrin family interacting with extracellular matrix components (12–15), supporting the concept of haptokinetic adhesion-dependent migration (1, 12).

Collective cell movement requires that several cells, grouped together by adhesive cell-cell contacts, generate front-rear asymmetry via unipolar ruffling in cells at the leading edge, whereas cells located at the trailing edge remain largely nonmotile (3, 4, 9). Such multicellular units constitute a larger-sized unit with reduced deformability, compared with individually migrating cells, and utilize yet unknown pathways of cell-cell communication. Polarized substrate interaction in tumor cell collectives has been shown for colon adenocarcinoma

sheets, which exhibit preferential expression of matrix metalloproteinases MMP-2 and MT1-MMP and focalized proteolytic degradation of gelatin substrate at the outward edges (16). However, how polarized cell-substrate interactions are established and which adhesion receptors are required for force generation in collective *versus* single-cell migration are unknown.

In the present study using primary melanoma explants, we show that collective tumor cell movement depends on  $\beta$ 1-integrin-mediated cell-matrix adhesion, force generation, and migration. Intriguingly, impairment of cluster cohesion resulted in the detachment and dissemination of amoeboid single cells, highlighting unexpected plasticity in tumor cell migration.

## MATERIALS AND METHODS

**Tumor Specimens.** Primary melanoma specimens were divided in the operation theater. The pathological diagnosis was established from paraffin sections by routine histology combined with immunohistochemistry for S100 protein, gp100, and MART-1. For primary explant culture, the malignant region of the explant was confirmed by frozen section, and immediately adjacent tissue portions were used for further explant culture in three-dimensional collagen lattices. In collagen, melanocytic cells within multicellular invasion zones and detached clusters were detected by immunohistochemistry using mAb<sup>4</sup> HMB45 (Dako, Hamburg, Germany) and anti-S100 mAb (Dako).

**Establishment of Primary Melanoma Cultures within Three-Dimensional Collagen Lattices.** Tumor samples were carefully dissected (maximum size, 1 × 1 × 1 mm) and incorporated into three-dimensional collagen lattices (1.67 mg/ml; Vitrogen bovine dermal collagen; Collagen Corp., Palo Alto, CA), as described previously (9). Explant cultures were monitored by bright-field microscopy for up to 6 weeks. Invasion zones or migrating cell clusters were defined as areas with more than four coherent cells and further monitored by time-lapse videomicroscopy for the exclusion of passively scattered nonmobile material or debris (9).

**Function-blocking Experiments.** For function blocking, adhesion-perturbing anti- $\beta$ 1 mAb 4B4 (Coulter, Hamburg, Germany; Ref. 17) and anti-E-cadherin mAb HECD-1 (Zymed, Berlin, Germany; Ref. 18) were used. Antibody 4B4 abrogates invasive melanoma cell migration within collagen lattices (15), and HECD-1 blocks E-cadherin-mediated cell-cell interactions, resulting in the scattering of epithelial cells from multicellular aggregates (16).

**Computer-assisted Cell Tracking.** Locomotion parameters were obtained by computer-assisted cell tracking and reconstruction of cell paths, as described previously (15, 19). In brief, the *X* and *Y* coordinates of six individual cells at different positions within the cluster were obtained for each step (step interval, 2–15 min) and reconstructed. Speed represented the total length of the calculated mean path of a cell group divided by time. Relative step angles of individual cell paths within a collective (corresponding to directional migration persistence) were calculated as relative deviation from each previous step and ranged from 0 (migration in a straight line) to 180 degrees (backward movement).

**Confocal Fluorescence and Reflection Microscopy.** For analysis of cluster interaction with collagen fibers and matrix remodeling, confocal reflection contrast and fluorescence microscopy (Leica TCS-4D; Bensheim, Germany) were performed as described previously (14, 20).

Received 7/5/01; accepted 1/23/02.

The costs of publication of this article were defrayed in part by the payment of page charges. This article must therefore be hereby marked *advertisement* in accordance with 18 U.S.C. Section 1734 solely to indicate this fact.

<sup>1</sup> This work was supported by the Gesellschaft für Biologische Krebsabwehr (F/117), the Felix-Wankel-Foundation, and the Erna-Graff-Foundation.

<sup>2</sup> Supplementary data for this article are available at *Cancer Research Online* (<http://cancerres.aacrjournals.org>).

<sup>3</sup> To whom requests for reprints should be addressed, at Department of Dermatology, University of Würzburg, Josef-Schneider-Strasse 2, 97080 Würzburg, Germany. E-mail: Peter.Fr@mail.uni-wuerzburg.de.

<sup>4</sup> The abbreviation used is: mAb, monoclonal antibody.

Table 1 Histological classification and in vivo infiltration depth of primary source melanoma: correlation with cluster development in explants cultured in vitro<sup>a</sup>

Classification	Sample number	Cluster frequency, <i>n</i> (%)
Histology		
SSM <sup>b</sup>	7	2/7 (29)
LMM	2	0/2 (0)
ALM	3	3/3 (100)
NM	1	1/1 (100)
Infiltration depth (mm)		
<1.69	5	2/5 (40)
1.7–3.6	6	2/6 (33)
>3.6	2	2/2 (100)

<sup>a</sup> Cultures were maintained for at least 2 weeks (average, 4–6 weeks).

<sup>b</sup> SSM, superficial spreading melanoma; LMM, lentigo-maligna melanoma; ALM, acro-lentiginous melanoma; NM, nodular melanoma.

## RESULTS

As monitored by explant culture in three-dimensional collagen lattices, 6 of 13 primary melanoma samples from different patients developed collective cell movement, as represented by multicellular invasion zones that progressed into migrating cell clusters. This migration type combined the maintenance of adhesive cell-cell junctions with invasive cell dissemination into tissue, as is frequently seen in melanoma histopathology (21, 22). Collective movement from melanoma explants was most prominent in samples from high-risk melanoma (tumor thickness >3.6 mm) as well as in samples from nodular and acro-lentiginous melanoma (Table 1). Cluster frequency, onset of migration (3–14 days), and morphological and migratory phenotypes were similar to clusters from rhabdomyosarcoma and epithelial cancer (9).

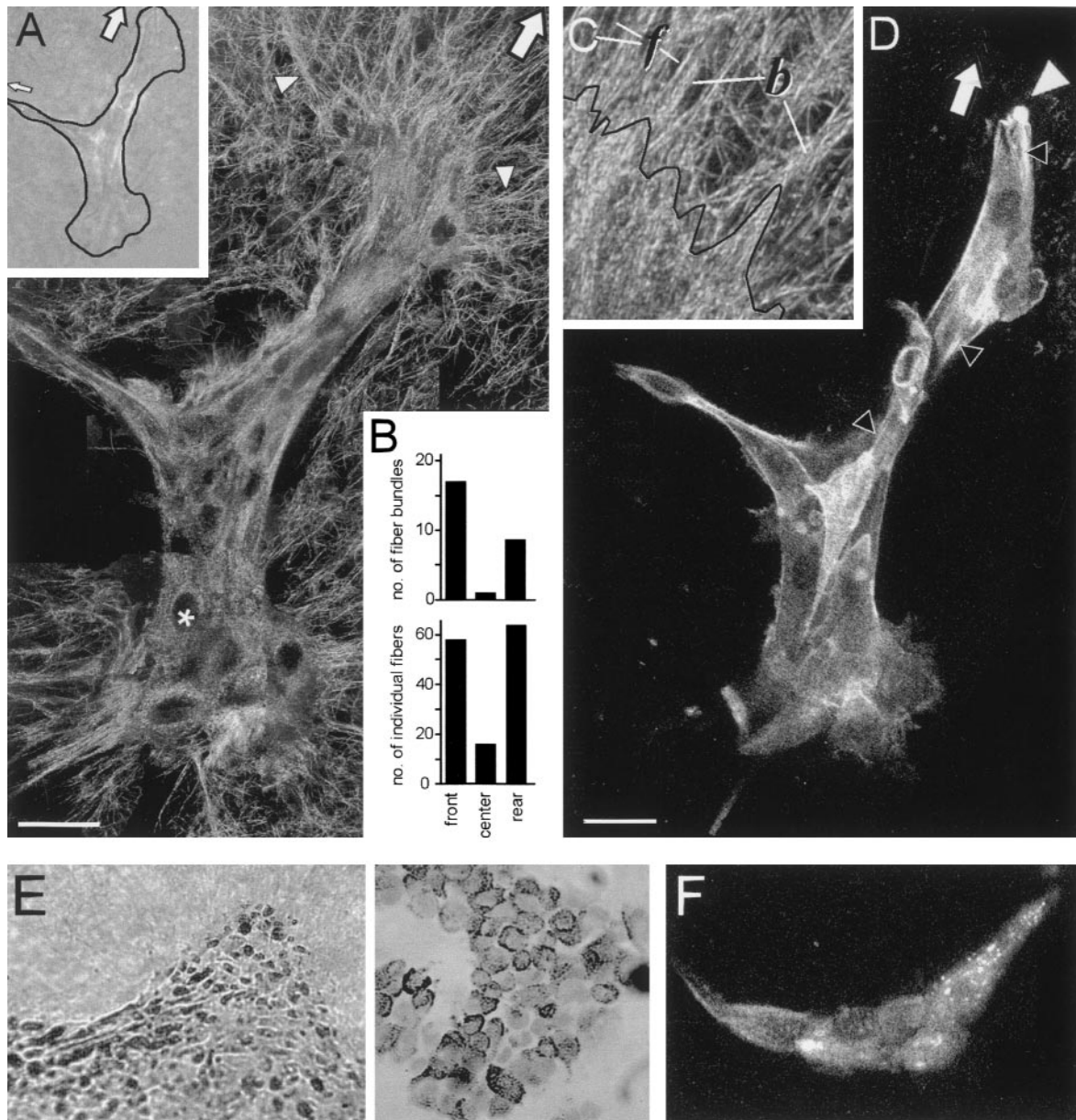


Fig. 1. Polarized cell-matrix interactions and F-actin distribution in migrating cluster. *A*, inset, as monitored by time-lapse videomicroscopy (black outline), one major and one minor leading edge (arrows) generated net migration toward the upper right-hand corner. *A*, confocal reflection microscopic image reconstructed from multiple frames and with extended focus in depth ( $\pm 3 \mu\text{m}$ ). White arrowheads, bundles of aligned collagen fibers; asterisk, reflection-negative cell nucleus. *B*, numbers of fibers and fiber bundles oriented toward the cluster body. *C*, high magnification of fiber traction zone at the leading edge. Solid black line, cell ruffles; *f*, individual fibers; *b*, fiber bundles. *D*, F-actin staining by FITC-phalloidin. White arrowhead, leading edge; black arrowheads, selected F-actin strands along traction lines and cell-cell junctions. Bars in *A* and *D*,  $35 \mu\text{m}$ . *E*, bright-field microscopy of cells containing pigmented granules in multicellular invasion zones; *F*, positive staining for mAb HMB45 in multicellular invasion zones.

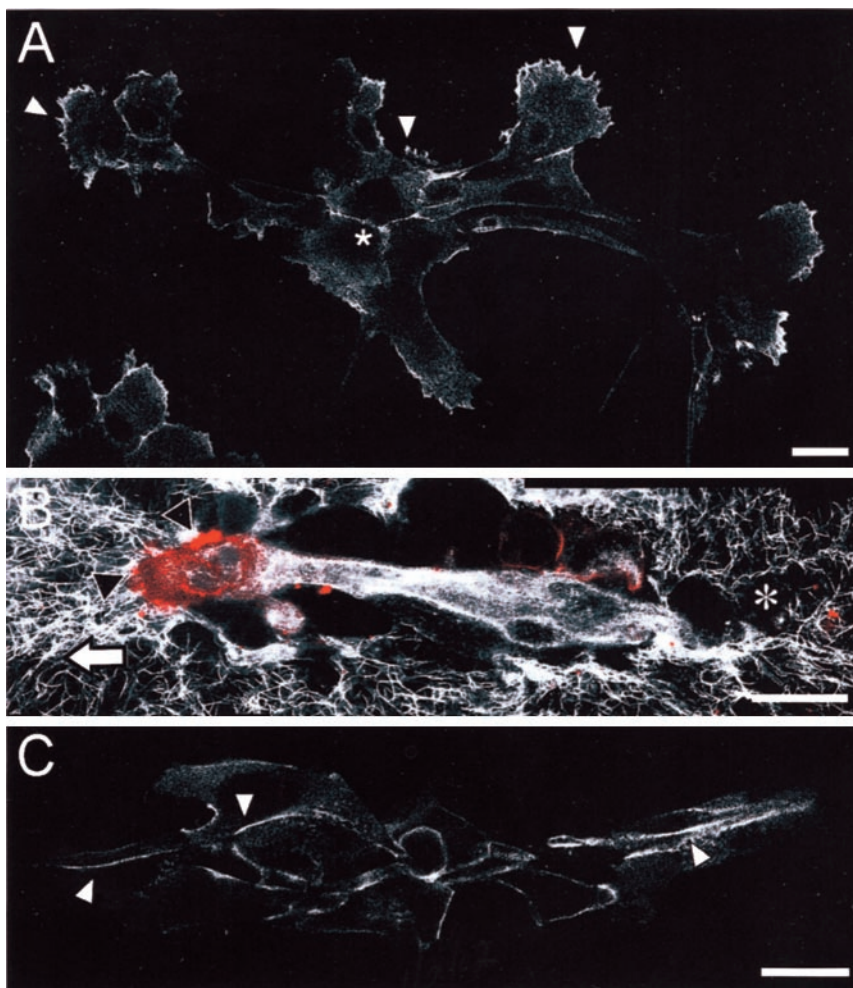


Fig. 2. Differential expression and redistribution of  $\beta 1$  integrins (A and B) and E-cadherin (C) in migrating melanoma clusters. A, clustered  $\beta 1$  integrins at ruffles at the leading edge(s). Asterisk, linear  $\beta 1$ -integrin staining at cell-cell contacts. B, selective  $\beta 1$ -integrin expression (red staining) at the leading edge in a subset of cells generating fiber alignment (black arrowheads). Clearance of collagen fibers is visible at the trailing edge (asterisk) and at lateral portions. C, linear E-cadherin staining at cell-cell junctions (white arrowheads), whereas E-cadherin was excluded from outward edges. Bars, 25  $\mu\text{m}$ .

**Asymmetry in Cell Matrix Interactions and Cytoskeletal Organization.** We first investigated how cluster polarity and movement corresponded to adhesive interactions with collagen fibers. The migratory direction was obtained by time-lapse videomicroscopy (Fig. 1A, inset, large arrow), followed by fixation and three-dimensional confocal reconstruction. As an indicator of high traction force, fiber alignment to thicker bundles converging toward the cluster body was preferentially detected at the leading edge and, less extensively, at the trailing edge (Fig. 1, A–C; compare with Fig. 2B). In contrast to bundles, individual fiber insertions were equally distributed at leading and trailing edges (Fig. 1, A–C). Although the three-dimensional nature of the collagen did not permit us to deduce traction forces, cluster-induced reorientation of collagen fibers (ranging up to 150–300  $\mu\text{m}$  in the forward direction) greatly exceeded fiber alignment generated by individual melanoma cells from previous studies (maximum of 50–100  $\mu\text{m}$  in the forward direction; Refs. 14, 15, 20).

As was apparent from time-lapse videorecordings (video 1) and reinforced by the structure of the actin cytoskeleton, migrating cell clusters behaved as asymmetric structural and functional units. The most prominent F-actin staining (Fig. 1D, white arrowhead) was located close to attachment and bundling sites at the leading edge, whereas more diffuse F-actin staining was present at the trailing edge. Cortical actin rims lacking stress fibers were present at most cell-cell junctions along traction lines over several adjacent cell bodies (Fig. 1D, black arrowheads), suggesting some degree of supracellular cytoskeletal organization. The presence of melanocytic cells within

multicellular invasion zones and detached clusters was confirmed by the presence of dark pigmented cells (Fig. 1E) as well as by positive staining for melanocytic marker HMB45 (Fig. 1F).

**Polarized Redistribution of  $\beta 1$  Integrins.** During cluster migration,  $\beta 1$  integrins comprising the major collagen receptors (i.e.,  $\alpha 1\beta 1$ ,  $\alpha 2\beta 1$ ,  $\alpha 3\beta 1$ ) were redistributed and clustered in ruffling microspikes along the leading edge(s) (Fig. 2A, white arrowheads). In contrast, nonclustered, linear  $\beta 1$ -integrin distribution was detected at some, but not all, cell-cell interactions (Fig. 2A, asterisk). In some clusters,  $\beta 1$ -integrin staining intensity was highly heterogeneous up to the exclusive expression of  $\beta 1$  integrins in a subset of cells in association with the leading fiber traction zone (Fig. 2B, black arrowheads). In contrast to  $\beta 1$  integrins, E-cadherin showed linear staining at cell-cell junctions only (Fig. 2C, arrowheads), in accordance with previous data on adenocarcinoma cell sheets (16). The extension of clusters clearly surpassed preformed matrix gaps, and a circumscribed matrix defect was detected at the trailing edge (Fig. 2B, asterisk), supporting the concept of proteolytic removal of matrix barriers during collective movement (16).

**Function of  $\beta 1$  Integrins in Cluster Migration.** To assess the function of  $\beta 1$  integrins in migratory force generation, migrating clusters were monitored before (endogenous baseline control) and after the addition of adhesion-perturbing anti- $\beta 1$ -integrin mAb 4B4. In two different explants, the addition of antibody 4B4 led to nearly complete abrogation of cluster migration (Fig. 3, A and B), whereas anti-E-cadherin mAb HECD-1 had no effect (Fig. 3C). In the absence of mAb, spontaneous baseline migration was maintained for at least 36 h (endogenous control; Fig. 3B). Together, polarized integrin

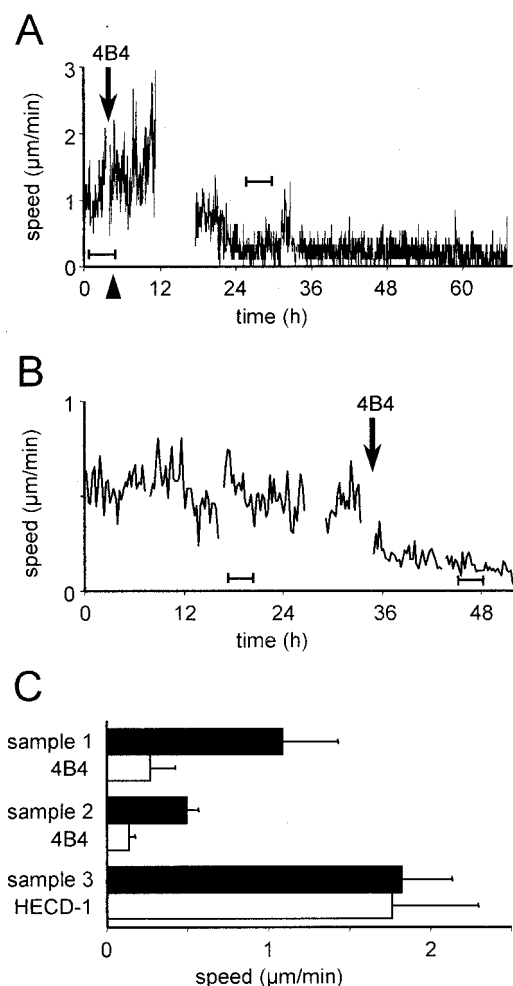


Fig. 3. Inhibition of cluster migration by adhesion-perturbing anti- $\beta$ 1-integrin mAb 4B4. *A* and *B*, cell tracking of six individual cells within the cluster over 3.5 h (*A*) or 36 h (*B*; internal baseline controls) before mAb 4B4 was added. Adhesion-blocking anti-E-cadherin mAb HECD-1 was used as control (*C*). Onset of changes in cluster migration 1–16 h after addition of mAb was in accordance with the distance of cluster location from the matrix-supernatant interface, supposedly reflecting variations in antibody diffusion time into the collagen. *C*, mean speed + SD (bars) before (■) and after addition of mAb (□) for the time frames indicated by horizontal bars in *A* and *B*.

engagement at the leading edge and mAb 4B4-induced abrogation of collective movement indicate an integrin-dependent, traction-driven mode of force generation.

**Front-Rear Asymmetry and Cluster Migration.** It became clear from the videorecordings that after the action of the  $\beta$ 1 integrins was blocked, impaired cluster migration involved complex changes in both cell-matrix and cell-cell interaction (video 1 in the supplementary material).<sup>2</sup> Collective baseline migration (Fig. 4*A*, *before*) resulted from stringent path coordination between individual cells at different locations within the cluster and a highly persistent mean path of the cluster (Fig. 4*B*), also shown by low directional deviation from step to step (relative step angles; Fig. 4*C*). As a first event 8–10 h after the addition of mAb 4B4, a second leading edge was developed by the former trailing edge, which pulled in the direction opposite to the previous direction of migration (Fig. 4*A* and video 2).<sup>2</sup> Consequently, path persistence was impaired (Fig. 4*B*), resulting in strongly oscillating relative step angles (Fig. 4*C*). Approximately 20 h after the addition of mAb 4B4, disruption of the cluster into two separate aggregates was complete (Fig. 4*A* and video 3).<sup>2</sup> Hence, after  $\beta$ 1-integrin function was disturbed and front-rear asymmetry was lost, previously nonmigratory subsets at the trailing edge were able to

initiate active migration within hours. As an end point, net cluster migration was lost (Fig. 4*A* and video 4),<sup>2</sup> resulting in scrambled uncoordinated cytoskeletal oscillations (“running on the spot”), whereas the residual capacity of cells to change position within the cluster (Fig. 4*B*, *top right panel*) and to interact with the collagen substrate (via  $\beta$ 1-integrin-independent mechanisms) remained intact.

**Loss of Homophilic Cell-Cell Contacts, Cell Detachment, and Amoeboid Single-Cell Crawling.** The sessile yet oscillatory state of the cluster gave rise to nonpolar outward ruffling and detachment of single cells, which migrated within the collagen at speeds of 0.2–0.6  $\mu\text{m}/\text{min}$  (Fig. 5, *A* and *B*; videos 3 and 4). Hence, previously nonmigrating cells located within the cluster retained a basic capacity to locomote individually, which however, appeared to have remained silenced as long as the cluster was intact.

Detached cells developed linear path segments alternating with sharp and tortuous changes in direction (Fig. 5*C*) and maintained an ellipsoid shape coupled to morphological adaptation along matrix structures (Fig. 5*D*, *panel a*, *asterisk*). Constriction rings developed at locations of narrow matrix constraints (Fig. 5*D*, *panel b*, *white arrowheads*), whereas no signs of prominent fiber bundling or proteolytic matrix remodeling were detected (Fig. 5*D*, *panel a*, *black arrowheads*). Hence, by altering the adhesive strength of cell-cell and/or cell-matrix interactions, neoplastic cells might be able to switch from one migration type to another.

## DISCUSSION

One major difference between individual and collective tumor cell movement is that collective migration requires a promigratory subset of cells at the leading edge. In morphogenic multicellular migration, cells at the leading margin of the zebrafish blastoderm were designated “forerunner cells” (8). In clusters, cells at the leading edge appear to function as “path generating” and “guiding” cells that are prevented from “forerunning” by stringent cell-cell contact within the cluster. Cells that form the leading edge may retain structural and functional properties not necessarily present in cells located at inner regions of the cluster. In principle, the functional specificity of guid-

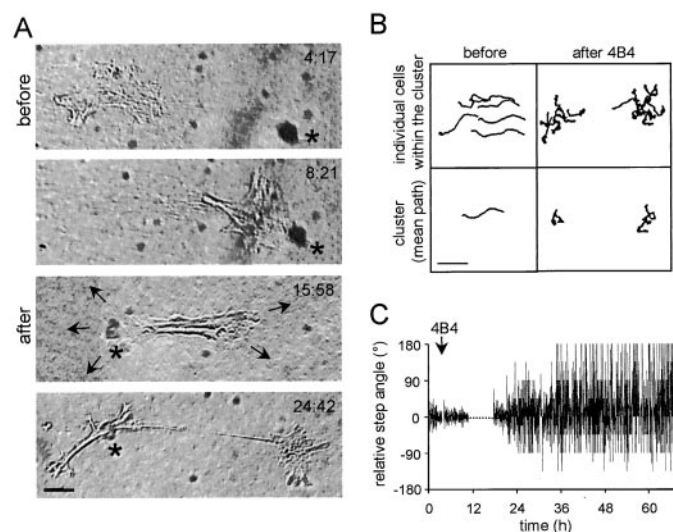


Fig. 4. Disruption of cluster integrity (*A*), coordination (*B*), and path persistence (*C*) after blocking of  $\beta$ 1 integrins. *A*, images from video recordings showing a nonmoving dark particle as reference point (*asterisk*), the time frame (hr:min), and counteracting ruffling edges (*arrows*). *B*, *X* and *Y* coordinates of six cells within the cluster (*top*) and mean trajectory (*bottom*) before (*left panels*) and after (*right panels*) addition of mAb 4B4. *Bars* in *A* and *B*, 100  $\mu\text{m}$ . *C*, loss of migratory persistence, as represented by relative step angles. *Negative Y values*, left turn; *positive Y values*, right turn.

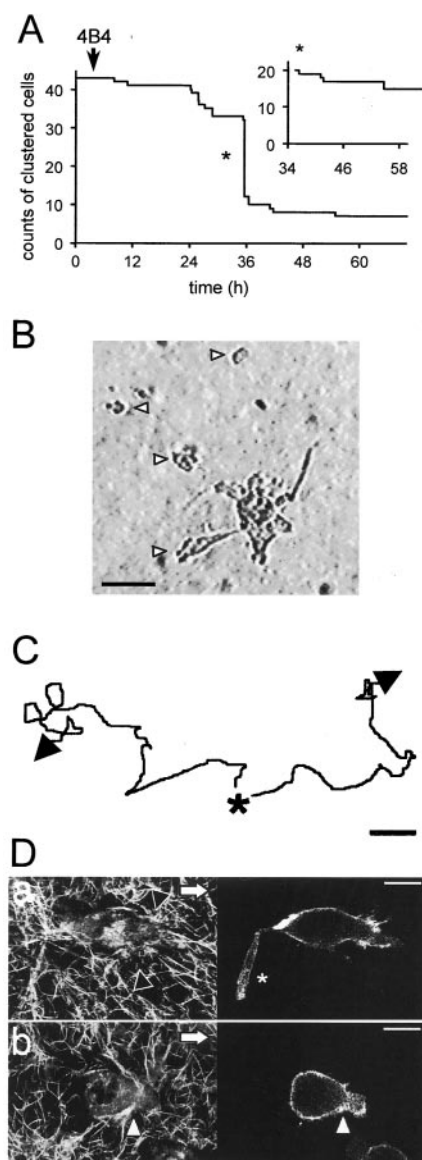


Fig. 5. Cluster disruption (A) and amoeboid single-cell crawling (B–D) after blocking of  $\beta 1$  integrins. A, cell loss from the cluster depicted in Fig. 4 after addition of mAb 4B4 (videos 3 and 4)<sup>2</sup> and splitting into two fragments (asterisk); inset, newly formed larger cluster. B, detachment of single amoeboid cells (arrowheads) from cluster remnant. Bar, 100  $\mu\text{m}$ . C, cell paths of two randomly selected cells after detachment. Bar, 20  $\mu\text{m}$ . D, amoeboid morphology of detached cells. Left, matrix structure; right,  $\beta 1$ -integrin staining; arrows, direction of migration. Panel a, polarized interaction with collagen fibers (black arrowheads) lacking matrix remodeling. Asterisk, retracting uropod along matrix fibers. Panel b, simple amoeboid shape and constriction ring (white arrowheads). Bars, 6  $\mu\text{m}$ .

ing cells could result from a genetic program, as detected in E-cadherin-mediated migration of ovarian follicle cells (slow border cells) within cell-rich tissue in embryonic *Drosophila melanogaster* (7). Alternatively, promigratory guiding activity could be a function of polarized integrin expression and engagement, as shown in the present study, as part of a temporary functional state maintained by graded cell-matrix interactions (13) and concomitant silencing of neighboring cells via cell-to-cell signaling. Clearly, more detailed studies are required on the integrin subsets, cell-cell adhesion, and cell-cell communication involved in collective movement. Although primary melanoma explants, as used in the present study, offer a natural source of highly invasive samples, some important restrictions reside in the limited availability of fresh source material as well as considerable donor-dependent heterogeneity in biological behavior. Hence, for reasons of efficiency and reproducibility, future studies

will additionally require the development of improved three-dimensional models using solid spheroids from established cell lines.

In melanoma clusters, the blocking of  $\beta 1$  integrins initiated a striking transition from multicellular migration to single-cell crawling. This process is reminiscent of the epithelial-to-mesenchymal transition that occurs when single epithelial cells scatter after treatment with SF/HGF or anti-E-cadherin antibody (16, 23). Blockage of the  $\beta 1$  integrins could directly interfere with integrin-mediated cell-cell cohesion by reducing homophilic integrin-integrin binding (24), by disturbing integrin binding to extracellular matrix components, such as fibronectin, contained along cell interphases (25), or by inducing changes in intracellular signaling toward other receptors that maintain homotypic cell-cell interaction in melanoma cells, such as N-cadherin (26) or L1 (27).

The transition of  $\beta 1$ -integrin-dependent collective movement to  $\beta 1$ -integrin-independent migration of single cells suggests that the forces involved in single-cell movement range below those required for migration of cell groups. The features of crawling cells after detachment from the cluster, *i.e.*, ellipsoid morphology, oscillatory path structure, the lack of matrix remodeling, and apparently low adhesive  $\beta 1$ -integrin-independent movement, are reminiscent of the amoeboid migration of T lymphocytes, which squeeze and crawl through matrix gaps present in three-dimensional collagen matrices (19, 28). A similar transition from fibroblast-like morphology toward amoeboid locomotor behavior was reported previously for neural crest cells after blockage of fibronectin-binding integrins (29), supporting the concept of residual migratory capacity after functional abrogation of certain integrin subsets. In conclusion, by altering the adhesive strength of cell-cell and/or cell matrix interactions, neoplastic cells may undergo transition from one migration program to another.

**Concept on Plasticity in Neoplastic Migration.** These results support a concept of diversity and adaptation in tumor cell migration within a three-dimensional tissue matrix. Collective cell movement in primary melanoma explants represents an efficient migration strategy that allows both active and passive translocation of heterogeneous sets of cells, thereby potentially promoting the dissemination of cells of different clonality and function within one functional unit. Importantly, once cell-substrate and/or cell-cell contacts are weakened, multicellular migration may convert to single-cell movement, representing the transition toward a secondary “salvage” migration strategy. Because cell migration may comprise diverse cellular and molecular mechanisms, future therapeutic targeting of the invasion cascade will require taking such migratory plasticity into consideration, *i.e.*, to further determine similarities and differences in collective *versus* single-cell movement as well as related transition stages.

## ACKNOWLEDGMENTS

We acknowledge Martina Jossberger for excellent technical assistance, Christian Rose for expert histological assessment, and Katarina Wolf for critical reading of the manuscript.

## REFERENCES

- Lauffenburger, D. A., and Horwitz, A. F. Cell migration: a physically integrated molecular process. *Cell*, 84: 359–369, 1996.
- Friedl, P., and Bröcker, E.-B. The biology of cell locomotion within three-dimensional extracellular matrix. *Cell. Mol. Life Sci.*, 57: 41–64, 2000.
- Vaughan, R. B., and Trinkaus, J. P. Movements of epithelial cell sheets *in vitro*. *J. Cell Sci.*, 1: 407–413, 1966.
- Kolega, J. The movement of cell clusters *in vitro*: morphology and directionality. *J. Cell Sci.*, 49: 15–32, 1981.
- Nabeshima, K., Moriyama, T., Asada, Y., Komada, N., Inoue, T., Kataoka, H., Sumiyoshi, A., and Koono, M. Ultrastructural study of TPA-induced cell motility: human well-differentiated rectal adenocarcinoma cells move as coherent sheets via localized modulation of cell-cell adhesion. *Clin. Exp. Metastasis*, 13: 499–508, 1995.

6. Armstrong, P. B. The control of cell motility during embryogenesis. *Cancer Metastasis Rev.*, *4*: 59–79, 1985.
7. Montell, D. J., Rorth, P., and Spradling, A. C. slow border cells, a locus required for a developmentally regulated cell migration during oogenesis, encodes *Drosophila* C/EBP. *Cell*, *71*: 51–62, 1992.
8. Cooper, M. S., and D'Amico, L. A. A cluster of noninvoluting endocytic cells at the margin of the zebrafish blastoderm marks the site of embryonic shield formation. *Dev. Biol.*, *180*: 184–198, 1996.
9. Friedl, P., Noble, P. B., Walton, P. A., Laird, D. E., Chauvin, P. J., Tabah, R. J., Black, M., and Zanker, K. S. Migration of coordinated cell clusters in mesenchymal and epithelial cancer explants *in vitro*. *Cancer Res.*, *55*: 4557–4560, 1995.
10. Trinkaus, J. P. Directional cell movement during early development of the teleost *Blennius pholis*: I. Formation of epithelial cell clusters and their pattern and mechanism of movement. *J. Exp. Zool.*, *245*: 157–186, 1988.
11. Palsson, E., and Othmer, H. G. A model for individual and collective cell movement in *Dictyostelium discoideum*. *Proc. Natl. Acad. Sci. USA*, *97*: 10448–10453, 2000.
12. Huttenlocher, A., Sandborg, R. R., and Horwitz, A. F. Adhesion in cell migration. *Curr. Opin. Cell Biol.*, *7*: 697–706, 1995.
13. Sheetz, M. P., Felsenfeld, D. P., and Galbraith, C. G. Cell migration: regulation of force on extracellular-matrix-integrin complexes. *Trends Cell Biol.*, *8*: 51–54, 1998.
14. Friedl, P., Maaser, K., Klein, C. E., Niggemann, B., Krohne, G., and Zanker, K. S. Migration of highly aggressive MV3 melanoma cells in 3 dimensional collagen lattices results in local matrix reorganization and shedding of  $\alpha 2$  and  $\beta 1$  integrins and CD44. *Cancer Res.*, *57*: 2061–2070, 1997.
15. Maaser, K., Wolf, K., Klein, C. E., Niggemann, B., Zanker, K. S., Brocker, E. B., and Friedl, P. Functional hierarchy of simultaneously expressed adhesion receptors: integrin  $\alpha 2 \beta 1$  but not CD44 mediates MV3 melanoma cell migration and matrix reorganization within three-dimensional hyaluronan-containing collagen matrices. *Mol. Biol. Cell*, *10*: 3067–3079, 1999.
16. Nabeshima, K., Inoue, T., Shimao, Y., Okada, Y., Itoh, Y., Seiki, M., and Koono, M. Front-cell-specific expression of membrane-type 1 matrix metalloproteinase and gelatinase A during cohort migration of colon carcinoma cells induced by hepatocyte growth factor/scatter factor. *Cancer Res.*, *60*: 3364–3369, 2000.
17. Morimoto, C., Letvin, N. L., Boyd, A. W., Hagan, M., Brown, H. M., Kornacki, M. M., and Schlossman, S. F. The isolation and characterization of the human helper inducer T cell subset. *J. Immunol.*, *134*: 3762–3769, 1985.
18. Shimoyama, Y., Hirohashi, S., Hirano, S., Noguchi, M., Shimosato, Y., Takeichi, M., and Abe, O. Cadherin cell-adhesion molecules in human epithelial tissues and carcinomas. *Cancer Res.*, *49*: 2128–2133, 1989.
19. Gunzer, M., Schäfer, A., Borgmann, S., Grabbe, S., Zänker, K. S., Bröcker, E.-B., Kämpgen, E., and Friedl, P. Antigen presentation in three-dimensional extracellular matrix: interactions of T cells with dendritic cells are dynamic, short lived, and sequential. *Immunity*, *13*: 323–332, 2000.
20. Friedl, P., and Brocker, E. B. Biological confocal reflection microscopy: reconstruction of three-dimensional extracellular matrix, cell migration, and matrix reorganization. In: D. P. Hader (ed.), *Image Analysis. Methods and Applications*. 2nd Ed., pp. 9–21. Boca Raton, FL: CRC Press, 2001.
21. Silye, R., Karayiannakis, A. J., Syrigos, K. N., Poole, S., van Noorden, S., Batchelor, W., Regele, H., Segá, W., Boesmueller, H., Krausz, T., and Pignatelli, M. E-Cadherin/catenin complex in benign and malignant melanocytic lesions. *J. Pathol.*, *186*: 350–355, 1998.
22. Li, G., and Herlyn, M. Dynamics of intercellular communication during melanoma development. *Mol. Med. Today*, *6*: 163–169, 2000.
23. Behrens, J., Weidner, K. M., Frixen, U. H., Schipper, J. H., Sachs, M., Arakaki, N., Daikuhara, Y., and Birchmeier, W. The role of E-cadherin and scatter factor in tumor invasion and cell motility. *EXS (Basel)*, *59*: 109–126, 1991.
24. Carter, W. G., Wayner, E. A., Bouchard, T. S., and Kaur, P. The role of integrins  $\alpha 2 \beta 1$  and  $\alpha 3 \beta 1$  in cell-cell and cell-substrate adhesion of human epidermal cells. *J. Cell Biol.*, *110*: 1387–1404, 1990.
25. Adams, J. C., and Watt, F. M. Changes in keratinocyte adhesion during terminal differentiation: reduction in fibronectin binding precedes  $\alpha 5 \beta 1$  integrin loss from the cell surface. *Cell*, *63*: 425–435, 1990.
26. Hsu, M., Andl, T., Li, G., Meinkoth, J. L., and Herlyn, M. Cadherin repertoire determines partner-specific gap junctional communication during melanoma progression. *J. Cell Sci.*, *113*: 1535–1542, 2000.
27. Silletti, S., Mei, F., Sheppard, D., and Montgomery, A. M. Plasmin-sensitive dibasic sequences in the third fibronectin-like domain of L1-cell adhesion molecule (CAM) facilitate homomultimerization and concomitant integrin recruitment. *J. Cell Biol.*, *149*: 1485–1502, 2000.
28. Friedl, P., Entschladen, F., Conrad, C., Niggemann, B., and Zanker, K. S. CD4+ T lymphocytes migrating in three-dimensional collagen lattices lack focal adhesions and utilize  $\beta 1$  integrin-independent strategies for polarization, interaction with collagen fibers and locomotion. *Eur. J. Immunol.*, *28*: 2331–2343, 1998.
29. Dufour, S., Duband, J. L., Humphries, M. J., Obara, M., Yamada, K. M., and Thiery, J. P. Attachment, spreading and locomotion of avian neural crest cells are mediated by multiple adhesion sites on fibronectin molecules. *EMBO J.*, *7*: 2661–2671, 1988.